Blockade of TGF-β inhibits mammary tumor cell viability, migration, and metastases

Rebecca S. Muraoka, … , Victor Koteliansky, Carlos L. Arteaga

Article **Development**

TGF-βs are potent inhibitors of epithelial cell proliferation. However, in established carcinomas, autocrine/paracrine TGF-β interactions can enhance tumor cell viability and progression. Thus, we studied the effect of a soluble Fc:TGF-β type II receptor fusion protein (Fc:TβRII) on transgenic and transplantable models of breast cancer metastases. Systemic administration of Fc:TβRII did not alter primary mammary tumor latency in MMTV-Polyomavirus middle T antigen transgenic mice. However, Fc:TβRII increased apoptosis in primary tumors, while reducing tumor cell motility, intravasation, and lung metastases. These effects correlated with inhibition of Akt activity and FKHRL1 phosphorylation. Fc:TβRII also inhibited metastases from transplanted 4T1 and EMT-6 mammary tumors in syngeneic BALB/c mice. Tumor microvessel density in a mouse dorsal skin window chamber was unaffected by Fc:TβRII. Therefore, blockade of TGF-β signaling may reduce tumor cell viability and migratory potential and represents a testable therapeutic approach against metastatic carcinomas.

Find the latest version:

https://jci.me/15234/pdf

Blockade of TGF-β inhibits mammary tumor cell viability, migration, and metastases

Rebecca S. Muraoka,[1,2] Nancy Dumont,[1] Christoph A. Ritter,[3] Teresa C. Dugger,[3] Dana M. Brantley,[3] Jin Chen,[2,3] Evangeline Easterly,[1] L. Renee Roebuck,[3] Sarah Ryan,[4] Philip J. Gotwals,[4] Victor Koteliansky,[4] and Carlos L. Arteaga[1,2,3]

[1]Department of Cancer Biology, Vanderbilt University School of Medicine, Nashville, Tennessee, USA
[2]Vanderbilt-Ingram Cancer Center, Nashville, Tennessee, USA
[3]Department of Medicine, Vanderbilt University School of Medicine, Nashville, Tennessee, USA
[4]Biogen Inc., Cambridge, Massachusetts, USA

Address correspondence to: Carlos L. Arteaga, Division of Oncology, Vanderbilt University School of Medicine, 2220 Pierce Avenue, 777 Preston Research Building, Nashville, Tennessee 27232-6307, USA. Phone: (615) 936-3524; Fax: (615) 936-1790; E-mail: carlos.arteaga@mcmail.vanderbilt.edu.

TGF-βs are potent inhibitors of epithelial cell proliferation. However, in established carcinomas, autocrine/paracrine TGF-β interactions can enhance tumor cell viability and progression. Thus, we studied the effect of a soluble Fc:TGF-β type II receptor fusion protein (Fc:TβRII) on transgenic and transplantable models of breast cancer metastases. Systemic administration of Fc:TβRII did not alter primary mammary tumor latency in MMTV-Polyomavirus middle T antigen transgenic mice. However, Fc:TβRII increased apoptosis in primary tumors, while reducing tumor cell motility, intravasation, and lung metastases. These effects correlated with inhibition of Akt activity and FKHRL1 phosphorylation. Fc:TβRII also inhibited metastases from transplanted 4T1 and EMT-6 mammary tumors in syngeneic BALB/c mice. Tumor microvessel density in a mouse dorsal skin window chamber was unaffected by Fc:TβRII. Therefore, blockade of TGF-β signaling may reduce tumor cell viability and migratory potential and represents a testable therapeutic approach against metastatic carcinomas.

J. Clin. Invest. **109**:1551–1559 (2002). doi:10.1172/JCI200215234.

Introduction

Tumor metastases are the result of a complex process that involves cellular migration, tumor vascularization, interactions with the microenvironment, intravasation into blood or lymphatic vessels, and cell survival at distant sites (1). TGF-β is a multifunctional cytokine involved in several of these processes (2, 3). The role of TGF-β in the biology of epithelial cells is complex. TGF-β potently inhibits the proliferation of epithelial cells (2). Transgenic mice that overexpress active TGF-β1 in mammary epithelium exhibit hypoplastic mammary glands that are resistant to oncogene- or carcinogen-induced mammary cancers (4–6). In a mouse skin model of chemical carcinogenesis, expression of TGF-β1 in keratinocytes suppresses the formation of benign skin tumors. Once tumors develop, however, TGF-β1 enhances tumor progression to a highly invasive spindle cell phenotype (7). Ha-Ras–induced mammary tumor cells secrete high levels of TGF-β and display highly invasive characteristics in vitro and in vivo (8). Introduction of dominant negative TGF-β type II receptors (TβRII) into these cells retards primary tumor and metastases formation and prevents epithelial-to-mesenchymal transition (EMT) (9). It appears, then, that many epithelial tumors escape growth inhibition by TGF-β, and TGF-β secretion by cancer and/or stromal cells may contribute to late tumor progression. Tumor TGF-β secretion may also indirectly favor metastatic progression by increasing extracellular matrix production/degradation, inducing tumor vascularization, and inhibiting effector mechanisms of immune surveillance (3, 10).

We have investigated the effect of TGF-β on breast cancer metastasis using a soluble chimeric protein composed of the extracellular domain of the TβRII and the Fc portion of the murine IgG$_1$ heavy chain (Fc:TβRII) (11). This chimera interferes with TGF-β binding to endogenous TGF-β receptors and has been shown to block TGF-β–induced fibrosis in vivo (12).

Methods

Fc:TβRII and transgenic mice. Fc:TβRII has been described previously (11). FVB MMTV-Polyomavirus middle T antigen (MMTV-PyV mT) mice (13) (The Jackson Laboratories, Bar Harbor, Maine, USA) were housed in the Animal Care Facility at Vanderbilt University following The American Association for the Accrediation of Laboratory Animal Care guidelines. Three-week-old transgenic mice were treated twice weekly with Fc:TβRII in PBS (5 mg/kg) by intraperitoneal injection. At 110 days, tissues were harvested and fixed in formalin or were snap-frozen. Serum levels of Fc:TβRII were measured by

immunoblot analysis using an anti-mouse IgG$_{2A}$-HRP (Southern Biotechnology Associates, Birmingham, Alabama, USA) against an Fc:TβRII standard curve (3.3–66 nM).

Histological analyses. Paraffin sections (5 μm) were stained with hematoxylin and eosin (Sigma-Aldrich, St. Louis, Missouri, USA). For immunohistochemistry, sections were treated as described (14), using Ab's against CD31 (1:100; Santa Cruz Biotechnology Inc., Santa Cruz, California, USA) or PyV mT antigen (pAb 701 [see ref. 15]; 1:50; provided by Steven Dilworth, Imperial Cancer Research Fund, London, United Kingdom). Immunohistochemical detection of bromodeoxyuridine (BrdU) incorporation and apoptosis was performed as described (16). Immunocytochemistry for Smad2, FKHRL1, vimentin, or β-catenin used Smad2 (1:100; Santa Cruz Biotechnology Inc.), FKHRL1 (1:100, Upstate Biotechnology Inc., Lake Placid, New York USA), vimentin (1:100; Santa Cruz Biotechnology Inc.), or β-catenin Ab's (Signal Transduction Laboratories, Lexington, Kentucky, USA), and Cy3-conjugated goat anti-rabbit IgG (Jackson ImmunoResearch Laboratories Inc., West Grove, Pennsylvania, USA).

Primary mammary tumor cell isolation and motility/invasion assays. Tumors from 110-day-old mice were digested (37°C, 4 hours) in 3 mg/ml collagenase A (Sigma-Aldrich), washed (PBS/10% FBS), and plated in DMEM:F12 (50:50; Life Technologies Inc., Carlsbad, California, USA), 5 ng/ml EGF, 5 ng/ml 17-β estradiol, 5 ng/ml progesterone, and 50 ng/ml insulin (all from Sigma-Aldrich). For wound closure assays, primary mammary tumor cells (PMTCs) were grown to confluence, treated with 80 pM (2 ng/ml) TGF-β1, 20 nM Fc:TβRII, or both, and wounded with a sterile circular rubber eraser (1 cm diameter). Cells were photographed at 0, 8, 16, 24, and 48 hours after wounding. The area of the circle enclosed by cells was determined using BioQuant (R&M Biometrics, Nashville, Tennessee, USA) software. Experiments were conducted with and without mitomycin C (1 μg/ml; Sigma-Aldrich). For invasion assays, PMTCs, 4T1, or EMT6 cells (10^4 each) were seeded in the upper chamber of transwells fitted with Matrigel-coated 8-μM pore-size polycarbonate filters (Corning Life Sciences, Acton, Massachusetts, USA). Lower chambers contained 2.5% serum with or without 20 nM Fc:TβRII. After 24 hours, cells were scraped from upper filter surfaces, and the cells on the lower surfaces were stained and counted.

Western blot analyses. Total protein (20 μg) was harvested and Western blot analysis performed as described previously (17) using the following Ab's: Shc, p85, Src, VEGF, and CD31 (all from Santa Cruz Biotechnology Inc.); Akt and Ser^{473} P-Akt (Transduction Laboratories, Lexington, Kentucky, USA); FKHRL1 and phospho-FKHRL1 (Upstate Biotechnology Inc.). Densitometric analysis was performed using ImageQuant software (Molecular Dynamics ImageQuant, Sunnyvale, California, USA).

^{125}I-TGF-β1 labeling. PMTCs were affinity labeled with 100 pM ^{125}I-TGF-β1 (NEN Life Science Products Inc., Boston, Massachusetts, USA) as described (18). In some cases, cross-linked cell lysates were precipitated with Ab (1 μg) against type I (V22) or type II (C16) TGF-β receptors (both from Santa Cruz Biotechnology Inc.). All samples were fractionated using 3–12% gradient SDS-PAGE, followed by autoradiography.

TGF-β reporter assays. PMTCs (0.5×10^6) were transfected with p3TP-Lux (2 μg) as described (19). After 48 hours, cells were treated for 6 hours with 80 pM TGF-β1, 20 nM Fc:TβRII, or both. Luciferase activity was determined using the Dual Luciferase Assay system (Promega Corp., Madison, Wisconsin, USA).

Measurement of secreted TGF-β. PMTCs (2×10^6) or primary mammary epithelial cells from wild-type mice were cultured for 24 hours in 3 ml of serum-free PMTC media. Conditioned medium was collected, concentrated to 0.5 ml, and TGF-β1 levels in media were determined using a TGF-β1 ELISA (R&D Systems Inc., Minneapolis, Minnesota, USA).

Intravasation assay. Circulating tumor cells in 110-day-old *PyV mT* mice were quantified as described in Wyckoff et al. (20). One milliliter of blood was collected by heart puncture and centrifuged (1200 *g*, 4°C, 5 minutes). The serum/buffy-coat layers were plated in 1 ml DMEM:F12 (50:50)/10% FBS. After 24 hours, the plates were washed with PBS to remove erythrocytes and nonadherent cells, and fresh DMEM:F12/10% FBS was replenished. After 7 days, colonies were stained with hematoxylin and counted.

Matrix metalloproteinase activity. Mouse tumors were harvested in 25 mM Tris-HCl, pH 7.8, 0.5 M NaCl, 1% NP-40, and EDTA-free protease inhibitor cocktail (Roche Diagnostics GmbH, Mannheim, Germany). Fifty micrograms of protein was analyzed for matrix metalloprotease-2/matrix metalloproteinase-9 (MMP-2/MMP-9) combined activity using the MMP Activity Assay Kit (Chemicon International Inc., Temecula, California, USA). The relative MMP activity per sample was compared with the MMP activity in 0.2 μg of recombinant MMP-2 (Chemicon International Inc.).

Transplants/metastases of 4T1 and EMT6 tumor cells. 4T1 or EMT6 cells (0.5×10^5) were injected into number 4 mammary glands of BALB/c virgin female mice. Mice were treated with Fc:TβRII as described above. After 10 days, primary tumors were resected. Lungs were harvested 8 weeks later, and surface metastases were counted.

Dorsal skin window assay. Window chambers were prepared in dorsal skin folds of female BALB/c mice as described (21). 4T1-green fluorescent protein (4T1-GFP) (22) cells (1,000 cells) were implanted in the chambers along with 1 mm^3 slow-release hydron pellets impregnated with Fc:TβRII (1 μg), normal mouse IgG (1 μg), or PBS. Growth of 4T1-GFP cells and vessels was observed within the window from days 0–15 using fluorescence and bright-field microscopy. On day 15, 100 μl of rhodamine-conjugated dextran (1 mg/ml) was injected intravenously to label functional vessels. Fluorescence was quantified using Scion Image software.
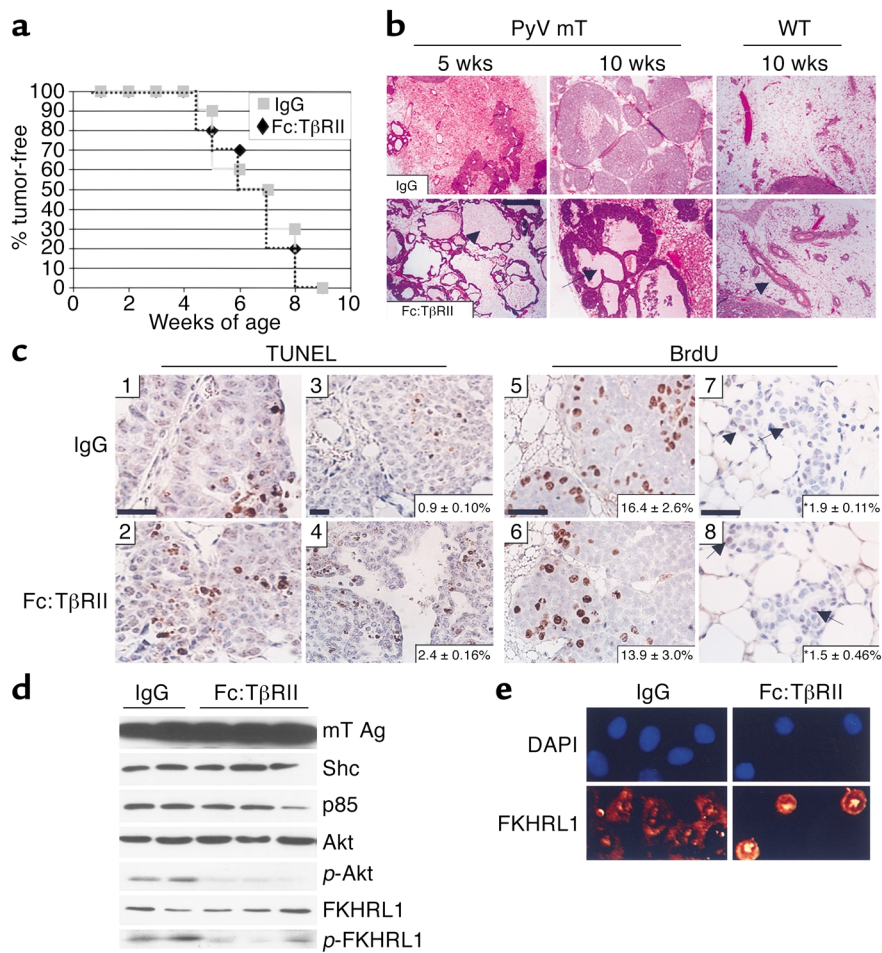
Figure 1
Tumor morphology, rate of apoptosis, and Akt signaling are altered by treatment with Fc:TβRII. (**a**) *MMTV/PyV mT* mice treated with Fc:TβRII or normal mouse IgG were examined twice weekly from 21 to 110 days of age. The initial observation of tumor onset is represented. (**b**) Histologic sections of tumors from 35- or 70-day-old transgenic or wild-type mice. Arrowheads indicate dilated ducts filled with secretory products. (**c**) TUNEL analysis (panels 1–4) of tumors harvested from 35- or 70-day-old mice treated with Fc:TβRII or IgG. $n = 6$ per condition. Quantification of percentage of apoptotic nuclei (bottom right corner of each panel) was calculated using the following equation: (number of TUNEL-positive nuclei in ×400 field) / (number of total nuclei in ×400 field). BrdU incorporation analysis (panels 5–8) of tumors harvested from 70-day-old *MMTV/PyV mT* or wild-type mice. Arrowheads in panels 7 and 8 indicate BrdU-positive nuclei. Quantification of percentage of BrdU-positive nuclei (bottom right corner of each panel) was calculated using the following equation: (number of BrdU-positive nuclei in ×400 field) / (number of total nuclei in ×400 field). *$P = 0.15$. Scale bars = 25 μm. (**d**) Tumor extracts harvested from 110-day-old transgenic mice were subjected to Western blot analysis using Ab's against the mT Ag, Shc, p85, Akt, *p*-Akt, FKHRL1, and *p*-FKHRL. (**e**) PMTCs were incubated with or without 20 nM Fc:TβRII for 6 hours and stained with a FKHRL1 Ab followed by staining with Cy3-conjugated anti-rabbit Ab. Nuclei were counterstained with DAPI.

Results

Soluble Fc:TβRII fusion protein increases mammary tumor cell apoptosis in MMTV-PyV mT transgenic mice. Transgenic mice that express the PyV mT antigen in mammary epithelium under the control of the MMTV-LTR promoter develop multifocal metastatic mammary tumors with a reported average tumor latency (T_{50}) of 53 days (13). Female MMTV-PyV mT mice were treated twice weekly with Fc:TβRII (5 mg/kg) or control IgG from 21 to 110 days of age. Mice treated with or without Fc:TβRII developed mammary tumors with a T_{50} of 56 days (Figure 1a). However, treatment with Fc:TβRII resulted in histologic alterations in the primary tumors. At 70 days, control glands displayed solid sheets of tumor cells. In contrast, Fc:TβRII-treated

mammary glands displayed cystic tumors containing secretions (Figure 1b). Mammary glands from wild-type FVB mice treated with Fc:TβRII also displayed increased ductal secretions, a result reminiscent of the precocious alveolar differentiation exhibited by transgenic mice expressing a dominant negative TβRII in mammary epithelium (23, 24). At 110 days, mice treated with Fc:TβRII displayed tumors in all 10 mammary glands, as did IgG-treated mice. Total tumor weight for mice treated with Fc:TβRII was 16.3 ± 3.2 g, compared with 17.9 ± 2.4 g for mice treated with IgG (unpaired Student *t* test, $P = 0.11$). Immunoblot analysis of 1:100 dilutions of mouse serum detected approximate Fc:TβRII levels between 6.6 and 66 nM (data not shown).
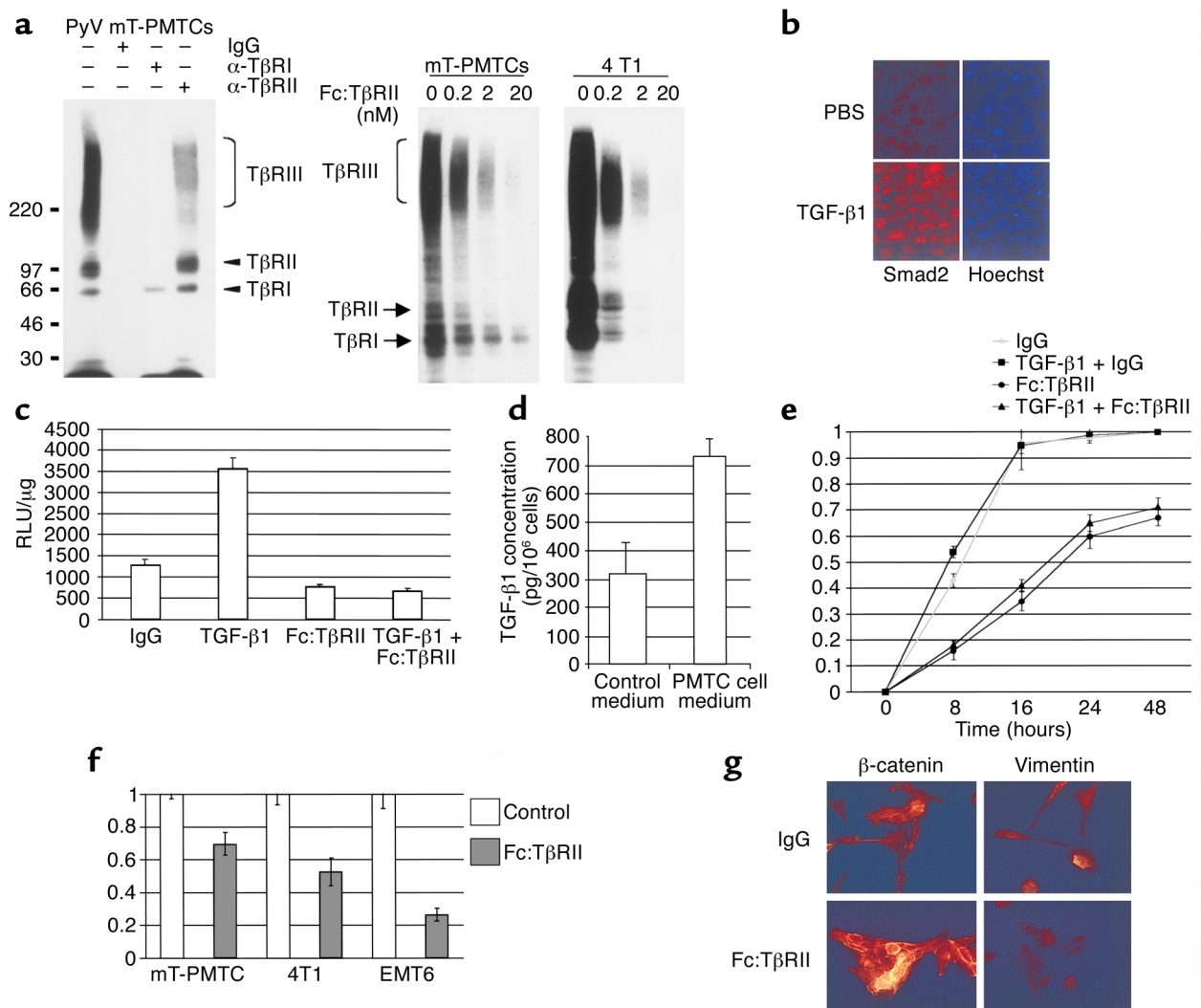
Figure 2
Fc:TβRII inhibits autocrine TGF-β signaling in PyV mT PMTCs. (**a**) Left panel: PMTCs were affinity labeled with ^{125}I-TGF-β1, resolved direct-ly (lane 1) or immunoprecipitated with the indicated TβR antibodies or IgG. Right panel: PMTCs and 4T1 cells were labeled with ^{125}I-TGFβ1 in the presence of the indicated concentrations of Fc:TβRII. (**b**) Immunofluorescent detection of Smad2 in PMTCs treated with PBS or TGF-β1. (**c**) PMTCs transfected with a 3TP-Lux were treated with Fc:TβRII, TGF-β1, or both. The results are presented as relative light units (RLUs)/μg of total protein.The values represent the average of 3 experiments performed in duplicate, ± SE. (**d**) PMTCs or PMECs were cul-tured in serum-free medium for 24 hours. Conditioned medium was collected and analyzed for TGF-β1 using ELISA. Results are shown as an average of 5 experiments, analyzed in triplicate. (**e**) PMTCs were grown to confluency and wounded. The results are presented as the percentage of the total area of the original wound enclosed by cells and represent the average ± SD obtained from five experiments, ana-lyzed in triplicate. (**f**) Transwell assays were performed using PMTCs, 4T1 cells, or EMT6 cells. The number of cells migrating to the lower side of the filter in controls was given the value of 1, such that migration of cells is represented as a fraction of control. Values shown are the average (± SE) of triplicate transwells in three experiments. (**g**) Immunocytochemical detection of β-catenin or vimentin in PMTCs cul-tured in the presence of the indicated factors. Representative photographs are shown.

Increased apoptosis was observed in tumors from 10-week-old mice treated with Fc:TβRII (2.4%) com-pared with controls (0.9%; $P = 0.024$; $n = 6$ per group; unpaired Student t test), as determined by TUNEL analysis (Figure 1c). However, treatment with Fc:TβRII did not alter the rate of tumor cell prolifer-ation as assessed by BrdU incorporation ($P = 0.08$; $n = 6$ per group). These results were confirmed in purified PMTCs harvested from 110-day-old MMTV-PyV mT mice. BrdU incorporation in PMTCs in cul-ture was not altered by TGF-β1 (14.3% ± 1.07%), by

Fc:TβRII (15.57% ± 1.52%), or by a combination of both (15.62% ± 1.52%), as compared with PMTCs treated with IgG (15.1% ± 1.15%).

Because mammary tumorigenesis induced by the PyV mT antigen has been shown to depend on the Shc, phosphatidylinositol-3 kinase (PI3K), and Src signal-ing pathways (25, 26), we investigated whether Fc:TβRII interfered with these mechanisms in the pri-mary tumors. Tumor contents of Shc and p85, the reg-ulatory subunit of PI3K, were unaffected by Fc:TβRII (Figure 1d). Src expression, detected by immunoblot

Table 1
Fc:TβRII inhibits tumor cell extravasation and lung metastases

Treatment:	WT	MMTV-*PyV mT*		
	Fc:TβRII	Fc:TβRII[A]	IgG[A]	*P* value
No. colonies	0	11.0 ± 2.6	71.8 ± 8.3	0.005
No. lung mets	0	2.9 ± 1.5	28.6 ± 4.1	0.004
Lung weight	0.32 ± 0.02 g	0.34 ± 0.02 g	0.42 ± 0.02 g	0.017
MMP (tissue)	2.16 ± 0.81	23.06 ± 2.89	29.46 ± 4.37	0.024
MMP (PMTCs)	N/A	2.55 ± 0.333	5.19 ± 0.87	0.008

The number of colonies derived from circulating blood of 70-day-old wild-type or *PyV mT* mice was quantified (see Figure 3b). Values shown are the average number of colonies derived per mouse, *n* = 6 per condition. The average number of macroscopic surface lung metastases per mouse was determined and counted by two different individuals (R.S. Muraoka and E. Easterly) in a blinded fashion; *n* >10 per condition. Wet lung weight was determined at time of death; *n* >10 per condition. Relative combined activity of MMP-2 and MMP-9 in mammary tissue extracts or cell lysates of purified PMTCs was determined using ELISA-based detection of MMP cleavage products (see Methods). Values represent the relative MMP activity in lysates compared with 0.2 μg of purified recombinant MMP-2. Values shown are the average of three independent experiments. *n* = 12 per condition (MMP: tissue); *n* = 8 per condition (MMP: PMTCs). [A]Statistical analysis performed using unpaired Student *t* test, comparing figures for Fc:TβRII and IgG. WT, wild-type; mets; metastases.

analysis, and in vitro kinase activity of Src were also unaffected (data not shown). Phosphorylation of Akt, a serine/threonine kinase whose activity is induced by PI3K (27), was diminished in Fc:TβRII-treated tumors approximately 2.4-fold. Phosphorylation of the Akt target FKHRL1, a Forkhead transcription factor that induces genes involved in cell death (28, 29), was also reduced 5.2-fold in Fc:TβRII-treated tumors. Consistent with previous reports showing that inhibition of Akt results in loss of FKHRL1 phosphorylation and translocation to the nucleus (28, 30), treatment with Fc:TβRII induced nuclear localization of FKHRL1 in PMTCs (Figure 1e).

PyV mT mammary tumor cells exhibit evidence of autocrine TGF-β signaling. Although proliferation of tumor cells was unaffected by Fc:TβRII, this was not due to lack of functional TGF-β receptors. PMTCs were affinity-labeled with ^{125}I-TGF-β1, resulting in three species with the characteristic mobility and molecular weight of type I, II, and III TGF-β receptors (Figure 2a). TGF-β binding was competed with nanomolar concentrations of Fc:TβRII. 4T1 mouse mammary tumor cells also expressed TGF-β receptors, whose interactions with labeled ligand were inhibited by Fc:TβRII. In PMTCs, exogenous TGF-β induced nuclear localization of Smad2 (Figure 2b), as well as transcription from the TGF-β–responsive reporter 3TP-Lux (Figure 2c). Both basal and TGF-β–induced reporter activity were blocked by Fc:TβRII (Figure 2c). These results suggest that TGF-β receptor–mediated signaling is intact in *PyV mT* mouse–derived cells. In addition, PMTCs synthesize and secrete close to 1 ng/ml/24 h of TGF-β1 (Figure 2d). Fc:TβRII impaired ligand-induced and basal motility of PMTCs (Figure 2e). The rate of wound closure was the same in the presence or absence of mitomycin C, suggesting that these effects were independent of cell proliferation (not shown). In transwell invasion assays, PMTCs, 4T1, and EMT6 BALB/c

mammary tumor cells migrated through extracellular matrix (Matrigel) to the opposite sides of filters. In each case, tumor cell migration was impaired by Fc:TβRII (Figure 2f). Cultured PMTCs treated with TGF-β1 and Fc:TβRII or with TGF-β1 alone were analyzed for expression of either β-catenin or vimentin using immunocytochemistry (Figure 2g). PMTCs treated with TGF-β1 and Fc:TβRII together displayed abundant β-catenin expression that was localized to the cell membranes. However, β-catenin expression was downregulated in PMTCs treated with TGF-β1. Vimentin expression, a marker of epithelial-to-mesenchymal transition, was observed in TGF-β1–treated PMTCs, but was not observed in PMTCs treated with Fc:TβRII and TGF-β together.

Blockade of TGF-β with Fc:TβRII reduces mammary tumor cell intravasation and lung metastases. At 110 days, lungs from transgenic mice were collected and examined for surface metastases. Lung surface metastases were observed in control mice and mice treated with Fc:TβRII. However, Fc:TβRII-treated mice displayed significantly lower wet lung weight (Table 1) and tenfold fewer lung surface metastases than controls (Figure 3a). All lung metastases expressed the MMTV-PyV mT transgene product as measured by immunohistochemistry (Figure 3a). Tumor cell intravasation was measured by collecting blood via atrial puncture and culturing the serum and buffy-coat layers (20). After 1 week, we determined the number of epithelial colonies (Figure 3b). Blood from wild-type mice produced no colonies. However, blood from control and Fc:TβRII-treated mice grew an average of 71.3 ± 8.3 and 11.0 ± 2.6 colonies per mouse, respectively (*n* = 6 per group; *P* < 0.009; unpaired student *t* test). Although we cannot rule out the possibility that Fc:TβRII affected the survival of circulating tumor cells, these results suggest that Fc:TβRII might interfere with the ability of tumor cells to migrate from the primary tumor and intravasate. Since TGF-β can also induce the expression of MMPs (10), we examined MMP activity in mammary tumor extracts. When normalized for protein content, the relative combined MMP-2 and MMP-9 activities were reduced in lysates prepared from Fc:TβRII-treated versus control tumors (Table 1). The relative levels of MMP activity were measured in extracts prepared from purified PMTCs treated in culture with Fc:TβRII or with control IgG. We found decreased MMP activity in Fc:TβRII-treated PMTC lysates compared with IgG-treated PMTC lysates, consistent with the hypothesis that Fc:TβRII may impair MMP activity in tumor cells.

To confirm that the antimetastatic effect of Fc:TβRII was not limited to *PyV mT* mice, we studied the effect of Fc:TβRII on 4T1 and EMT6 mammary tumor cell metastases. These transplantable mouse
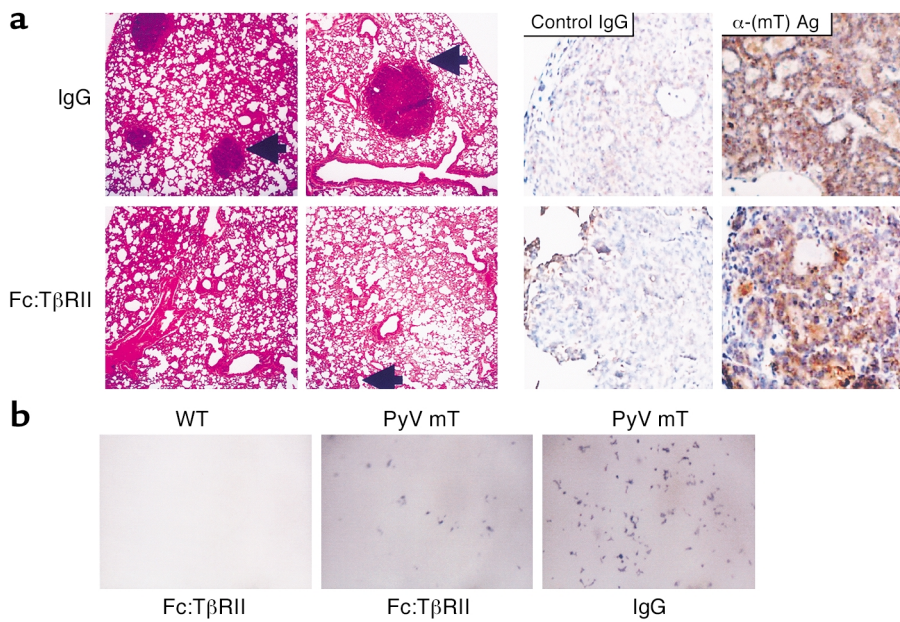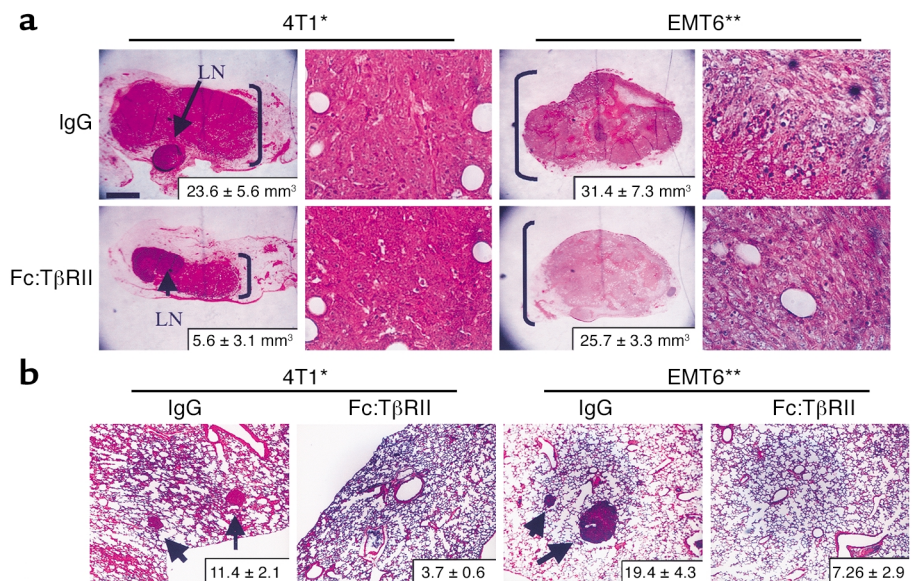
a

IgG

Fc:TβRII

Control IgG   α-(mT) Ag

b

WT   PyV mT   PyV mT

Fc:TβRII   Fc:TβRII   IgG

Figure 3

Fc:TβRII decreases *PyV mT* mouse tumor cell intravasation and lung metastases. (**a**) Hematoxylin and eosin–stained lung sections (left panels) or mT Ag immunohistochemical analysis (right panels) of lungs harvested from 110-day-old *PyV mT* mice. Arrows point to lung metastases. Immunohistochemistry was performed using normal mouse IgG or pAb 762 against middle T antigen [α-(mT) Ag]. (**b**) Photomicrographs of hematoxylin-stained tumor cell colonies harvested from the blood of 110-day-old wild-type or *PyV mT* mice treated with normal mouse IgG or Fc:TβRII.

tumor cells express high levels of TGF-β ligands and receptors and exhibit enhanced motility in response to exogenous TGF-β (19). Furthermore, expression of a dominant negative truncated TβRII in 4T1 cells markedly restricted lung metastases (31). 4T1 or EMT6 cells (0.5×10^5) were implanted into the mammary glands of virgin 6-week-old BALB/c mice. Mice were treated twice weekly with Fc:TβRII, and primary tumors were resected after 10 days. Fc:TβRII was continued for 8 additional weeks. After only three doses of Fc:TβRII, 4T1 and EMT6 tumors were smaller than controls (Figure 4a), suggesting that tumor growth in vivo is retarded by TGF-β blockade. Although this result is in contrast with the results obtained using Fc:TβRII in the MMTV-PyV mT mice, the difference may be due to differential effects of Fc:TβRII on an

experimental tumor derived from metastatic tumors (i.e., 4T1 and EMT6) compared with a tumor that has evolved de novo from preneoplastic mammary epithelial cells (i.e., MMTV-PyV mT mammary glands). We found BrdU incorporation was not significantly different in 4T1 tumors treated with Fc:TβRII (17.9% ± 2.4%) compared with IgG-treated 4T1 tumors (18.4% ± 2.2%; $P = 0.14$; unpaired student t test), suggesting that tumor cell proliferation was not affected by Fc:TβRII. Mice treated with Fc:TβRII had 3.1-fold ($P < 0.006$) and 2.6-fold ($P < 0.002$; unpaired Student t test) fewer 4T1 and EMT6 lung metastases, respectively, compared with IgG-treated mice (Figure 4b). In addition to the lungs, 4T1 cells have been reported to metastasize to other sites in BALB/c mice, including the liver. Mice treated

Figure 4

Fc:TβRII inhibits 4T1 and EMT6 primary tumor size and lung metastases. Tumor cells (0.5×10^5 4T1 or EMT6) were injected into the mammary fat pad of BALB/c mice. Mice were treated twice weekly with Fc:TβRII. (**a**) After 10 days, primary tumors were resected. Arrows indicate the lymph nodes of the number 4 mammary gland. The average tumor volume ($n = 8$ per condition), calculated by the formula vol-ume = width² × length/2, is indicated in the lower right corner. *$P = 0.011$; **$P = 0.05$. (**b**) Lungs were collected at 8 weeks and examined for lung surface metastases. Arrows indicate metastases. The average number of metastases per mouse is shown in the bottom right corner of each panel ($n = 8$ per condition). *$P = 0.026$; **$P = 0.034$.

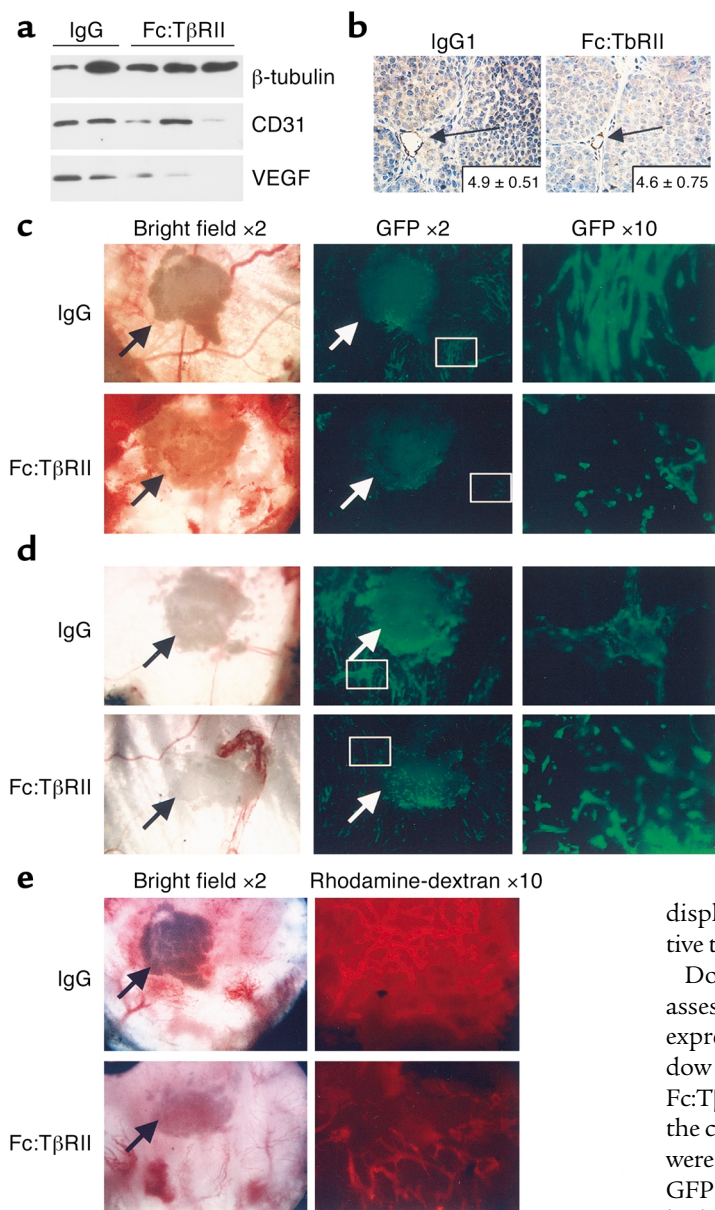
a

4T1*   EMT6**

IgG

LN   23.6 ± 5.6 mm³   31.4 ± 7.3 mm³

Fc:TβRII

LN   5.6 ± 3.1 mm³   25.7 ± 3.3 mm³

b

4T1*   EMT6**

IgG   Fc:TβRII   IgG   Fc:TβRII

11.4 ± 2.1   3.7 ± 0.6   19.4 ± 4.3   7.26 ± 2.9

a
IgG   Fc:TβRII

β-tubulin
CD31
VEGF

b
IgG1   Fc:TbRII

4.9 ± 0.51   4.6 ± 0.75

c
Bright field ×2   GFP ×2   GFP ×10

IgG

Fc:TβRII

d
IgG

Fc:TβRII

e
Bright field ×2   Rhodamine-dextran ×10

IgG

Fc:TβRII

Figure 5

Fc:TβRII alters tumor cell density and invasiveness but not tumor angiogenesis. (**a**) Tumor lysates from *PyV mT* mice were subjected to Western blot analysis using Ab's against β-tubulin, CD31, or VEGF. The VEGF isoform shown is mouse VEGF-A$_{120}$, migrating at 14 kDa. (**b**) Immunohisto-chemical detection of CD31 in tumors harvested from 110-day-old *MMTV/PyV mT* mice treated with normal mouse IgG or Fc:TβRII. The average number of vessels per ×400 field is indicated in the lower-right corner of each panel. (*n* = 10 random tumor fields from three mice per condition.) Dorsal skin window analysis of in vivo tumor angiogenesis. One hundred 4T1-GFP cells were implanted into dorsal window chambers in BALB/c mice along with Fc:TβRII-, IgG-, or PBS-releasing pellets on day 0. Arrows indicate location of the pellet. On day 15, mice were administered rhodamine-con-jugated dextran. Digital photomicrographs were taken on days 5 (**c**), 10 (**d**), and 15 (**e**) under green field (to visualize 4T1-GFP tumor cells), red field (to visualize the rhodamine-labeled vasculature), and bright field. Relative tumor densi-ty was calculated using the following equation: (average number of fluorescent pixels per sample in Fc:TβRII group)/(average number of fluorescent pixels per sample in IgG con-trol group and PBS control group combined). The relative vascular density was determined using the following equa-tion: (number of fluorescent pixels in test sample)/(number of fluorescent pixels in IgG and PBS controls).

with Fc:TβRII displayed fewer surface liver metastases (4.4 ± 1.2) compared with IgG-treated mice (6.4 ± 1.31; *P* < 0.04. unpaired Student *t* test, *n* = 5).

Antimetastatic effect of soluble Fc:TβRII is not associated with inhibition of tumor angiogenesis. TGF-β may promote angiogenesis via multiple mechanisms, including increased production of VEGF and recruitment of perivascular pericytes, among others (32). Western analysis of primary tumor extracts from control or Fc:TβRII-treated MMTV-PyV mT mice demonstrated the presence of VEGF-A isoforms at 42, 27, and 14 kDa (Figure 5a and data not shown). Expression of CD31, a marker for endothelial cells, was observed in tumors treated with or without Fc:TβRII. Quantification by immunohistochemistry of the number of CD31-posi-tive vessels in situ was similar in tumors treated or not treated with Fc:TβRII (*P* = 0.19, *n* = 5; Figure 5b). Similarly, Fc:TβRII-treated 4T1 and EMT6 tumors displayed no differences in the number of CD31-posi-tive tumor vessels compared with controls (not shown).

Dorsal skin window assays (21) were performed to assess early stages of angiogenesis. 4T1 tumor cells expressing GFP (22) were implanted into a dorsal win-dow chamber. A hydron pellet impregnated with Fc:TβRII, PBS, or normal mouse IgG was implanted in the chamber. 4T1 tumor formation and vascularization were monitored over a 15-day period. At day 5, the 4T1-GFP cells in the window chamber containing a control hydron pellet were present at a higher density than those in the presence of an Fc:TβRII pellet. Upon higher mag-nification, Fc:TβRII-treated cells were rounded com-pared with the spindle-shaped 4T1-GFP cells in control chambers. At day 10, Fc:TβRII-treated cells remained as rounded, single cells (Figure 5c). At day 14, mice were administered rhodamine-dextran intravenously to visu-alize vascularization of tumors. There were no differ-ences in vascularity of control versus Fc:TβRII-treated 4T1-GFP tumors as measured by rhodamine-fluorescent pixels. However, tumor density determined by the num-ber of GFP-fluorescent pixels was decreased in the Fc:TβRII-treated mice (Figure 5d and Table 2), suggest-ing that Fc:TβRII may have an effect on tumor cells inde-pendent of any detectable effect on endothelial cell recruitment and/or new vessel formation.

Discussion
Blockade of TGF-β signaling with soluble Fc:TβRII inhibited the formation of distant metastases in three

Table 2
Vascular density is not reduced by Fc:TβRII

	Day 5		Day 10		Day 15	
	IgG	Fc:TβRII	IgG	Fc:TβRII	IgG	Fc:TβRII
Tumor density	1,742 ± 141	597 ± 96	4,796 ± 274	865 ± 174	22,988 ± 1,412	14,765 ± 1,633
Vascular density	N/A	N/A	N/A	N/A	27,861 ± 1,955	26,433 ± 2,720

The density of 4T1 tumor cells in dorsal skin window chambers was quantified at the indicated time points as the average number of GFP-generated fluorescent pixels per ×20 field (see Figure 5, c and d) using Scion Image software, *n* = 6 per condition. The vascular density of 4T1 tumors in dorsal skin window chambers was quantified as the average number of rhodamine-generated fluorescent pixels per ×20 field (see Figure 5d) using Scion Image software, *n* = 6 per condition.

experimental models of breast cancer. Although responsive to exogenous TGF-β (Figure 2), inhibition of TGF-β signaling using Fc:TβRII did not alter cellular proliferation in the tumor cells used in this study, neither in vitro nor in vivo (Figure 1c), suggesting that the antimetastatic effects of Fc:TβRII in vivo were independent of tumor cell proliferation. However, treatment with Fc:TβRII inhibited tumor cell motility (Figure 2) and intravasation (Figure 3), inhibited MMP activity in tumors (Table 1), and increased cancer cell apoptosis in situ (Figure 1). These data suggest that TGF-β signaling contributes to metastasis (33) and that Fc:TβRII (or other mechanisms of systemic inhibition of TGF-β1 signaling) may be an effective treatment for the prevention of tumor cell metastasis. These data are consistent with studies in which inactivating mutations in the *TβRII* gene in colon cancers correlate with a low invasive potential; introduction of exogenous TβRII into these colon cancer cells increased tumor cell invasion (9). Approximately 90% of colon cancers with microsatellite instability have inactivating mutations of TβRII (34), which correlates with longer patient survival (35), implying that loss of TGF-β signaling may limit systemic metastases.

Mammary tumors from mice treated with Fc:TβRII displayed a higher rate of apoptosis than that observed for control-treated tumors. Interestingly, we found that Fc:TβRII inhibited phosphorylation of Akt on serine 473. Phosphorylation on serine 473 is required for maximal Akt kinase activity resulting in subsequent phosphorylation of multiple downstream targets of Akt, such as p21, p27, GSK3β, IKKα, and FKHRL1. Phosphorylation of FKHRL1 by Akt results in the cytoplasmic retention (i.e., nuclear exclusion) of FKHRL1, thus preventing FKHRL1-induced transcription of death-associated genes. Therefore, inhibition of Akt might conceivably result in enhanced nuclear localization of FKHRL1 and increased cell death. The data reported herein suggest that, by inhibiting the phosphorylation/activation of Akt, Fc:TβRII treatment resulted in increased nuclear localization of FKHRL1. This correlated with an increase in the number of apoptotic nuclei in situ in tumors treated with Fc:TβRII. These data are consistent with reports published previously demonstrating the reported induction of PI3K by TGF-β (42). TGF-β–neutralizing Ab's are known to inhibit phosphorylation of Akt at serine 473 in 4T1

and EMT6 cells (19). More recently, it was shown that TGF-β enhances epithelial cell survival via Akt-induced phosphorylation and nuclear exclusion of FKHRL1 (30). Therefore, inhibition of TGF-β–induced AKT activity by Fc:TβRII may enhance tumor cell death and limit metastatic progression.

The data presented cannot rule out the possibility that Fc:TβRII-mediated blockade of TGF-β signaling in immune effector cells might lead to eradication of tumor, as demonstrated recently in mice expressing dominant negative TβRII in CD4^{+} and CD8^{+} T cells (36). It is difficult to compare the results presented herein with the powerful results reported by Gorelick and Flavell (36), who used a highly aggressive, poorly immunogenic, transplantable model of melanoma, while our studies examined the endogenous formation of breast tumors from preneoplastic mammary epithelium. This difference may present differences in the mechanisms by which the immune system recognize tumor cells. Additionally, TGF-β may have different effects on tumor progression at different stages of tumorigenesis. TGF-β is thought to act as a tumor suppressor early in tumorigenesis, perhaps by inhibiting cell proliferation. Later in tumor progression, however, TGF-β may not inhibit tumor cell proliferation and may actually enhance tumor cell invasion and the tumor microenvironment, while inhibiting tumoricidal activity of the immune system, thus enhancing tumor progression. It is conceivable that Fc:TβRII would interfere with each of these effects of TGF-β on tumor progression. Nonetheless, the studies showing inhibition of TGF-β signaling in T cells, taken together with data presented herein, demonstrate a beneficial effect in tumor metastasis prevention by inhibition of TGF-β signaling.

Our studies suggest that inhibition of TGF-β signaling using Fc:TβRII may not interfere with tumor angiogenesis in vivo. This finding is in contrast to other studies using TGF-β inhibitors (10, 32). TGF-β is predominantly involved in smooth muscle cell differentiation and migration leading to pericyte recruitment and vessel stabilization (37). However, the majority of intratumor neovessels lack periendothelial smooth muscle cells (38), potentially explaining our inability to detect a reduction of in situ vascular density in endogenously arising tumors and in dorsal skin window chambers.

In summary, the mechanisms by which TGF-β can promote late stages of tumor progression represent testable molecular targets for novel interventions like Fc:TβRII. Our results suggest that inhibition of TGF-β signaling results in decreased metastasis of mammary tumors by impairing invasion, migration, and cellular survival. The lack of any obvious toxicity in mice treated with Fc:TβRII for 12 weeks suggests that Fc:TβRII or other inhibitors of the TGF-β signaling pathway may prove to be powerful antimetastatic therapies.

1. Hanahan, D., and Weinberg, R.A. 2000. The hallmarks of cancer. *Cell*. **100**:57–70.
2. Massague, J. 1998. TGF-beta signal transduction. *Annu. Rev. Biochem.* **67**:753–791.
3. Derynck, R., Akhurst, R.J., and Balmain, A. 2001. TGF-beta signaling in tumor suppression and cancer progression. *Nat. Genet.* **29**:117–129.
4. Pierce, D.F., Jr., et al. 1993. Inhibition of mammary duct development but not alveolar outgrowth during pregnancy in transgenic mice expressing active TGF-beta 1. *Genes Dev.* **7**:2308–2317.
5. Jhappan, C., et al. 1993. Targeting expression of a transforming growth factor beta 1 transgene to the pregnant mammary gland inhibits alveolar development and lactation. *EMBO J.* **12**:1835–1845.
6. Pierce, D.F., Jr., et al. 1995. Mammary tumor suppression by transforming growth factor beta 1 transgene expression. *Proc. Natl. Acad. Sci. USA.* **92**:4254–4258.
7. Cui, W., et al. 1996. TGFbeta1 inhibits the formation of benign skin tumors, but enhances progression to invasive spindle carcinomas in transgenic mice. *Cell*. **86**:531–542.
8. Oft, M., et al. 1996. TGF-beta1 and Ha-Ras collaborate in modulating the phenotypic plasticity and invasiveness of epithelial tumor cells. *Genes Dev.* **10**:2462–2477.
9. Oft, M., Heider, K.H., and Beug, H. 1998. TGFbeta signaling is necessary for carcinoma cell invasiveness and metastasis. *Curr. Biol.* **8**:1243–1252.
10. Dumont, N., and Arteaga, C.L. 2000. Transforming growth factor-beta and breast cancer: tumor promoting effects of transforming growth factor-beta. *Breast Cancer Res.* **2**:125–132.
11. Cosgrove, D., et al. 2000. Integrin alpha1beta1 and transforming growth factor-beta1 play distinct roles in alport glomerular pathogenesis and serve as dual targets for metabolic therapy. *Am. J. Pathol.* **157**:1649–1659.
12. George, J., Roulot, D., Koteliansky, V.E., and Bissell, D.M. 1999. In vivo inhibition of rat stellate cell activation by soluble transforming growth factor beta type II receptor: a potential new therapy for hepatic fibrosis. *Proc. Natl. Acad. Sci. USA.* **96**:12719–12724.
13. Guy, C.T., Cardiff, R.D., and Muller, W.J. 1992. Induction of mammary tumors by expression of Polyomavirus middle T oncogene: a transgenic mouse model for metastatic disease. *Mol. Cell Biol.* **12**:954–961.
14. Brantley, D.M., et al. 2000. Dynamic expression and activity of NF-kappaB during post-natal mammary gland morphogenesis. *Mech. Dev.* **97**:149–155.
15. Dilworth, S.M., and Horner, V.P. 1993. Novel monoclonal antibodies that differentiate between the binding of pp60c-src or protein phosphatase 2A by Polyomavirus middle T antigen. *J. Virol.* **67**:2235–2244.
16. Muraoka, R.S., et al. 2001. Cyclin-dependent kinase inhibitor p27(Kip1) is required for mouse mammary gland morphogenesis and function. *J. Cell Biol.* **153**:917–932.
17. Lenferink, A.E., Busse, D., Flanagan, W.M., Yakes, F.M., and Arteaga, C.L. 2001. ErbB2/neu kinase modulates cellular p27(Kip1) and cyclin D1 through multiple signaling pathways. *Cancer Res.* **61**:6583–6591.
18. Dumont, N., O'Connor-McCourt, M.D., and Philip, A. 1995. Transforming growth factor-beta receptors on human endometrial cells: identification of the type I, II, and III receptors and glycosyl-phosphatidylinositol anchored TGF-beta binding proteins. *Mol. Cell Endocrinol.* **111**:57–66.
19. Bakin, A.V., Tomlinson, A.K., Bhowmick, N.A., Moses, H.L., and Arteaga, C.L. 2000. Phosphatidylinositol 3-kinase function is required for transforming growth factor beta-mediated epithelial to mesenchymal transition and cell migration. *J. Biol. Chem.* **275**:36803–36810.
20. Wyckoff, J.B., Jones, J.G., Condeelis, J.S., and Segall, J.E. 2000. A critical step in metastasis: in vivo analysis of intravasation at the primary tumor. *Cancer Res.* **60**:2504–2511.
21. Huang, Q., et al. 1999. Noninvasive visualization of tumors in rodent dorsal skin window chambers. *Nat. Biotechnol.* **17**:1033–1035.
22. Lin, P., et al. 1997. Inhibition of tumor angiogenesis using a soluble receptor establishes a role for Tie2 in pathologic vascular growth. *J. Clin. Invest.* **100**:2072–2078.
23. Bottinger, E.P., Jakubczak, J.L., Haines, D.C., Bagnall, K., and Wakefield, L.M. 1997. Transgenic mice overexpressing a dominant-negative mutant type II transforming growth factor beta receptor show enhanced tumorigenesis in the mammary gland and lung in response to the carcinogen 7,12-dimethylbenz-[a]-anthracene. *Cancer Res.* **57**:5564–5570.
24. Gorska, A.E., Joseph, H., Derynck, R., Moses, H.L., and Serra, R. 1998. Dominant-negative interference of the transforming growth factor beta type II receptor in mammary gland epithelium results in alveolar hyperplasia and differentiation in virgin mice. *Cell Growth Differ.* **9**:229–238.
25. Guy, C.T., Muthuswamy, S.K., Cardiff, R.D., Soriano, P., and Muller, W.J. 1994. Activation of the c-Src tyrosine kinase is required for the induction of mammary tumors in transgenic mice. *Genes Dev.* **8**:23–32.
26. Webster, M.A., et al. 1998. Requirement for both Shc and phosphatidylinositol 3′ kinase signaling pathways in Polyomavirus middle T-mediated mammary tumorigenesis. *Mol. Cell Biol.* **18**:2344–2359.
27. Datta, S.R., Brunet, A., and Greenberg, M.E. 1999. Cellular survival: a play in three Akts. *Genes Dev.* **13**: 2905–2927.
28. Brunet, A., et al. 1999. Akt promotes cell survival by phosphorylating and inhibiting a Forkhead transcription factor. *Cell*. **96**:857–868.
29. Nakamura, N., et al. 2000. Forkhead transcription factors are critical effectors of cell death and cell cycle arrest downstream of PTEN. *Mol. Cell Biol.* **20**:8969–8982.
30. Shin, I., Bakin, A.V., Rodeck, U., Brunet, A., and Arteaga, C.L. 2001. Transforming growth factor beta enhances epithelial cell survival via Akt-dependent regulation of FKHRL1. *Mol. Biol. Cell.* **12**:3328–3339.
31. McEarchern, J.A., et al. 2001. Invasion and metastasis of a mammary tumor involves TGF-beta signaling. *Int. J. Cancer*. **91**:76–82.
32. Pepper, M.S. 1997. Transforming growth factor-beta: vasculogenesis, angiogenesis, and vessel wall integrity. *Cytokine Growth Factor Rev.* **8**:21–43.
33. Miettinen, P.J., Ebner, R., Lopez, A.R., and Derynck, R. 1994. TGF-beta induced transdifferentiation of mammary epithelial cells to mesenchymal cells: involvement of type I receptors. *J. Cell Biol.* **127**:2021–2036.
34. Markowitz, S., et al. 1995. Inactivation of the type II TGF-beta receptor in colon cancer cells with microsatellite instability. *Science*. **268**:1336–1338.
35. Thibodeau, S.N., Bren, G., and Schaid, D. 1993. Microsatellite instability in cancer of the proximal colon. *Science*. **260**:816–819.
36. Gorelik, L., and Flavell, R.A. 2001. Immune-mediated eradication of tumors through the blockade of transforming growth factor-beta signaling in T cells. *Nat. Med.* **7**:1118–1122.
37. Hirschi, K.K., Rohovsky, S.A., and D'Amore, P.A. 1998. PDGF, TGF-beta, and heterotypic cell-cell interactions mediate endothelial cell-induced recruitment of 10T1/2 cells and their differentiation to a smooth muscle fate. *J. Cell Biol.* **141**:805–814.
38. Benjamin, L.E., Golijanin, D., Itin, A., Pode, D., and Keshet, E. 1999. Selective ablation of immature blood vessels in established human tumors follows vascular endothelial growth factor withdrawal. *J. Clin. Invest.* **103**:159–165.